

All-optical injection and control of spin and electrical currents in quantum wells

Ali Najmaie, R. D. R. Bhat, and J. E. Sipe

Department of Physics, University of Toronto, 60 St. George Street, Toronto, Ontario, Canada M5S 1A7

(Received 16 April 2003; published 30 October 2003)

We show that quantum interference between one- and two-photon absorption can be used to inject spin currents, with or without an accompanying electrical current, in unbiased semiconductor quantum well structures. The directions in which the electrical and spin currents are injected can be coherently controlled, with a relative phase parameter of the optical fields as the control parameter. We characterize the currents for an unstrained quantum well and a quantum well under biaxial compressive strain using the Luttinger-Kohn model; we work out particular examples. If compressive strain is used to appropriately rearrange the subbands, then a degree of spin polarization of the spin currents higher than possible in bulk GaAs can be achieved and maintained even for photon energies well above the band gap.

DOI: 10.1103/PhysRevB.68.165348

PACS number(s): 78.20.Ls, 42.65.-k, 72.25.Fe, 73.63.Hs

I. INTRODUCTION

The control and manipulation of the spin degree of freedom of electrons in semiconductor structures has received much attention in recent years and may be an important component of the future data storage and processing protocols. Since the 1970s it has been known that, due to spin-orbit interactions, spin-polarized carriers can be generated in semiconductors through optical excitation with circularly polarized optical fields.¹ Using a bias voltage, this spin population can be dragged to produce a spin-polarized current;^{2,3} such spin currents always have a net electrical current accompanying them. The degeneracy of the heavy- and light-hole bands at the Γ point in bulk semiconductors, such as GaAs, implies that any excitation across the band gap occurs from both the heavy- and light-hole bands; this leads to a reduction in the degree of spin polarization of the injected carriers. This degeneracy is lifted in a quantum well semiconductor structure due to confinement and, further, via strain, thus leading to a higher degree of spin polarization of the injected carriers.⁴

Recently it has been shown⁵⁻⁷ that quantum mechanical interference between one- and two-photon excitation in bulk semiconductors can be used to induce spin currents in semiconductors without the need of a bias voltage or magnetic field. In some configurations *pure* spin currents can be generated, where no *net* electrical current is involved. Furthermore, the direction of injection of the electrical and spin currents can be controlled using a relative phase parameter of the optical fields. The experimental verification of injection and control of the pure spin current has been performed by injecting carriers in the plane of a quantum well structure.⁶

In this paper we present a detailed account of coherent injection of electrical and spin *currents* in the plane of a GaAs quantum well and its control through quantum mechanical interference using a relative phase parameter of the beams responsible for one- and two-photon excitations. We further study the effects of biaxial compressive strain on the injected currents. Our goal here is to study the effects of these physical parameters on the injected currents in a general way. In a future publication we will apply this framework to address particular experimental results⁶ in detail.

We begin in Sec. II with the model used to describe the electronic states of a strained quantum well. In Sec. III, we use Fermi's golden rule to describe and formulate susceptibilities describing the one, two, and interference components of the optical excitations; we also introduce quantities that are used to represent the degree of spin polarization of the spin currents and the velocity of the injected carriers. In Sec. IV we present the results for different polarization configurations, with the optical fields propagating along the growth axis. In Sec. V we summarize our results and conclude.

II. QUANTUM WELL STATES

We consider an isolated GaAs quantum well grown in the $\langle 001 \rangle$ direction, which we take as the quantization axis z , and set the boundaries of the quantum well at $\pm L/2$. We use two Hamiltonians for the energy dispersion and eigenstates of the subbands, one for the valence subbands and another for the conduction subbands; these we now describe. All the calculations neglect interactions between carriers, except to the extent they are described in the effective single-electron model of the bands. In the present work, we consider a quantum well subjected to photons with energies below that needed to couple the bound states to the continuum states associated with electrons or holes moving out of the well; the coherent control of spin currents due to this coupling is subject of a future report. Indeed, we consider here excitation energies up to only about 100 meV above the band gap of the quantum well; for these energies there are no contributions from the barrier material and we approximate the barriers as infinite.

A. Valence subbands

We begin with the 4×4 Luttinger-Kohn Hamiltonian^{8,9,11} to describe the valence subbands. The split-off subbands, lying about 350 meV below the top of the valence subband, are neglected since we consider photons with $2\hbar\omega \ll 350$ meV.¹² In the presence of (001) biaxial strain,¹⁰ the Luttinger-Kohn Hamiltonian is modified by the appearance of Bir-Pikus strain terms⁹ and takes the form

$$H = - \begin{bmatrix} P+Q & L & M & 0 \\ L^\dagger & P-Q & 0 & M \\ M^\dagger & 0 & P-Q & -L \\ 0 & M^\dagger & -L^\dagger & P+Q \end{bmatrix} + V(z), \quad (1)$$

where the potential $V(z)$ describes the quantum well, with

$$P(\hat{\mathbf{k}}) = \frac{\hbar^2 \gamma_1}{2m_0} \hat{k}^2 + P_\epsilon,$$

$$Q(\hat{\mathbf{k}}) = \frac{\hbar^2 \gamma_2}{2m_0} (\hat{k}_x^2 + \hat{k}_y^2 - 2\hat{k}_z^2) + Q_\epsilon,$$

$$L(\hat{\mathbf{k}}) = \frac{-i\hbar^2 \sqrt{3} \gamma_3}{m_0} (\hat{k}_x - i\hat{k}_y) \hat{k}_z,$$

$$M(\hat{\mathbf{k}}) = \frac{\sqrt{3}\hbar^2 \gamma_2}{2m_0} (\hat{k}_x^2 - \hat{k}_y^2) - i \frac{\sqrt{3}\hbar^2 \gamma_3}{m_0} \hat{k}_x \hat{k}_y,$$

and where we use the differential operator $\hat{\mathbf{k}} \equiv -i\nabla$. The adjoint differential operators appearing here are defined in the usual way,

$$\int [L^\dagger(\hat{\mathbf{k}}) \phi_2(\mathbf{r})]^* \phi_1(\mathbf{r}) d\mathbf{r} = \int \phi_2^*(\mathbf{r}) [L(\hat{\mathbf{k}}) \phi_1(\mathbf{r})] d\mathbf{r},$$

where of course $\hat{\mathbf{k}}^\dagger = \hat{\mathbf{k}}$. The coefficients $\{\gamma_1, \gamma_2, \gamma_3\}$ are the Luttinger parameters;⁸ in this paper the dispersion of the valence bands of the quantum well is assumed to be isotropic in the $k_x k_y$ plane, which is achieved by setting $\gamma_2 = \gamma_3 \equiv \gamma$. The strain factors $P_\epsilon = 2a_v[(c_{11} - c_{12})/c_{11}]\epsilon$ and $Q_\epsilon = b[(c_{11} + 2c_{12})/c_{11}]\epsilon$ involve the stiffness tensor coefficients c_{ij} and the deformation potential constants a_v and b of the crystal structure.⁹ The strain parameter ϵ describes the change in the lattice constant of the crystal; the ratio of the lattice constant in the strained crystal, a' , to that in the unstrained crystal, a , is given by $a'/a = (1 + \epsilon)$. Thus for $\epsilon > 0$ the strain is tensile, and for $\epsilon < 0$ it is compressive.

Within the usual envelope function approximation, the Hamiltonian (1) acts on the space of envelope function vectors $F(\mathbf{r})$,

$$F(\mathbf{r}) = \begin{bmatrix} F_1(\mathbf{r}) \\ F_2(\mathbf{r}) \\ F_3(\mathbf{r}) \\ F_4(\mathbf{r}) \end{bmatrix},$$

where the $F_i(\mathbf{r})$ are complex functions, in terms of which the full spinor wave function $\psi(\mathbf{r})$ can be written as

$$\begin{aligned} \psi(\mathbf{r}) = & F_1(\mathbf{r}) \mu_{(3/2,3/2)}(\mathbf{r}) + F_2(\mathbf{r}) \mu_{(3/2,1/2)}(\mathbf{r}) \\ & + F_3(\mathbf{r}) \mu_{(3/2,-1/2)}(\mathbf{r}) + F_4(\mathbf{r}) \mu_{(3/2,-3/2)}(\mathbf{r}). \end{aligned}$$

Here the $\mu_{(i,j)}(\mathbf{r})$ are spinor functions of \mathbf{r} , the coordinate representations of the Γ_8 Bloch functions $\{|\frac{3}{2}, \frac{3}{2}\rangle, |\frac{3}{2}, \frac{1}{2}\rangle, |\frac{3}{2}, -\frac{1}{2}\rangle, |\frac{3}{2}, -\frac{3}{2}\rangle\}$ at $\mathbf{k}_t = 0$, using the convention

$$\mu_{(\frac{3}{2}, \frac{3}{2})}(\mathbf{r}) = \frac{1}{\sqrt{2}} [X(\mathbf{r}) + iY(\mathbf{r})] \alpha,$$

$$\mu_{(\frac{3}{2}, \frac{1}{2})}(\mathbf{r}) = \frac{i}{\sqrt{6}} \{[X(\mathbf{r}) + iY(\mathbf{r})] \beta - 2Z(\mathbf{r}) \alpha\},$$

$$\mu_{(\frac{3}{2}, -\frac{1}{2})}(\mathbf{r}) = \frac{1}{\sqrt{6}} \{[X(\mathbf{r}) - iY(\mathbf{r})] \alpha + 2Z(\mathbf{r}) \beta\},$$

$$\mu_{(\frac{3}{2}, -\frac{3}{2})}(\mathbf{r}) = \frac{i}{\sqrt{2}} [X(\mathbf{r}) - iY(\mathbf{r})] \beta,$$

where $X(\mathbf{r})$, $Y(\mathbf{r})$, and $Z(\mathbf{r})$ are the functions associated with the representation Γ_{15} of the zinc-blende point group T_d , and α and β are the spinor basis functions:

$$\alpha = \begin{pmatrix} 1 \\ 0 \end{pmatrix}, \quad \beta = \begin{pmatrix} 0 \\ 1 \end{pmatrix}.$$

To solve for the eigenstates of the Hamiltonian (1) we must solve the eigenvalue problem

$$HF(\mathbf{r}) = EF(\mathbf{r}), \quad (2)$$

with eigenvalue E , subject to the appropriate boundary conditions. Consider first solutions of Eq. (2) in the well (or in principle in the barrier) bulk material, where $V(z)$ is a constant. Then solutions of the form $F_i(\mathbf{r}) = F_i \exp(i\mathbf{k} \cdot \mathbf{r})$ can be sought, where we write $\mathbf{k} = k_t + \hat{\mathbf{z}} k_z$, with $\mathbf{k}_t = k_t(\hat{\mathbf{x}} \cos \phi + \hat{\mathbf{y}} \sin \phi)$. The determinant following from Eq. (2) in the usual way leads to the dispersion equation

$$E = -P(\mathbf{k}) \pm [Q^2(\mathbf{k}) + L(\mathbf{k})L^\dagger(\mathbf{k}) + M(\mathbf{k})M^\dagger(\mathbf{k})]^{1/2}, \quad (3)$$

where, for example, to construct the function $L^\dagger(\mathbf{k})$ we take the differential operator $L^\dagger(\hat{\mathbf{k}})$ introduced above and replace the differential operator $\hat{\mathbf{k}}$ by the vector \mathbf{k} . Fixing E and \mathbf{k}_t at real values, we solve Eq. (3) for k_z , which may be complex. In general there are four solutions $k_z = \pm k_L, \pm k_H$. Taking linear combinations of these in different regions of constant $V(z)$, in general we seek solutions that satisfy the appropriate boundary conditions at the interfaces at $\pm L/2$ and at infinity; for these the envelope function components take the form $F(\mathbf{r}) = e^{i(k_x x + k_y y)} f(z)$,

TABLE I.

Quantum well width	L (nm)	10
Lattice constant	a_0 (Å)	5.6533
Energy gap at 0 K	E_g (eV)	1.519
Matrix element parameter	$\frac{2m_e}{\hbar^2} P_0 ^2$ (eV)	25.7
Deformation potential	a_c (eV)	-7.17
Deformation potential	a_v (eV)	1.16
Deformation potential	b (eV)	-1.7
Stiffness coefficient	c_{11} (10^{11} dyn/cm ²)	11.879
Stiffness coefficient	c_{12} (10^{11} dyn/cm ²)	5.376
Effective mass	m_c/m_e	0.067
Luttinger parameter	γ_1	6.85
Luttinger parameter	$\gamma = (\gamma_2 + \gamma_3)/2$	2.5

$$\begin{aligned}
 f(z) = & B_1 \begin{bmatrix} 0 \\ M(\mathbf{k}_t) \sin(k_L z) \\ iL(\mathbf{k}_t + \hat{\mathbf{z}}k_L) \cos(k_L z) \\ R_1(\mathbf{k}_t + \hat{\mathbf{z}}k_L) \sin(k_L z) \end{bmatrix} \\
 & + B_2 \begin{bmatrix} 0 \\ M(\mathbf{k}_t) \sin(k_H z) \\ iL(\mathbf{k}_t + \hat{\mathbf{z}}k_H) \cos(k_H z) \\ R_1(\mathbf{k}_t + \hat{\mathbf{z}}k_H) \sin(k_H z) \end{bmatrix} \\
 & + B_3 \begin{bmatrix} M(\mathbf{k}_t) \cos(k_H z) \\ 0 \\ -R_2(\mathbf{k}_t + \hat{\mathbf{z}}k_H) \cos(k_H z) \\ -iL^\dagger(\mathbf{k}_t + \hat{\mathbf{z}}k_H) \sin(k_H z) \end{bmatrix} \\
 & + B_4 \begin{bmatrix} M(\mathbf{k}_t) \cos(k_L z) \\ 0 \\ -R_2(\mathbf{k}_t + \hat{\mathbf{z}}k_L) \cos(k_L z) \\ -iL^\dagger(\mathbf{k}_t + \hat{\mathbf{z}}k_L) \sin(k_L z) \end{bmatrix},
 \end{aligned}$$

for $R_1(\mathbf{k}) = Q(\mathbf{k}) - P(\mathbf{k}_t + \hat{\mathbf{z}}k_z) - E$ and $R_2(\mathbf{k}) = Q(\mathbf{k}) + P(\mathbf{k}) + E$. The constants B_i for $i = 1-4$ are also evaluated from application of the boundary conditions. The boundary conditions yield a determinant with zeros corresponding to valence subband energies $E(\mathbf{k}_t)$. Parameters used in our calculations are shown in Table I.⁹ In Fig. 1, we show the valence states used in our calculations.

To identify the eigenvectors in a convenient form, it is useful to exploit other symmetries of the Hamiltonian. The Hamiltonian (1) is invariant under time reversal symmetry, and since terms linear in the components of \mathbf{k}_t are ignored, reflection with respect to the xy plane is a good symmetry operation;¹¹ the operator associated with this is $\sigma = \exp(-i\pi J_z)I$ (not to be confused with the Pauli spin matrices), where J_z is the generator of rotation around the z axis and I is the space inversion operator. Following Andreani *et al.*¹¹ we shall denote the eigenvalues of σ by *parity*, not to be

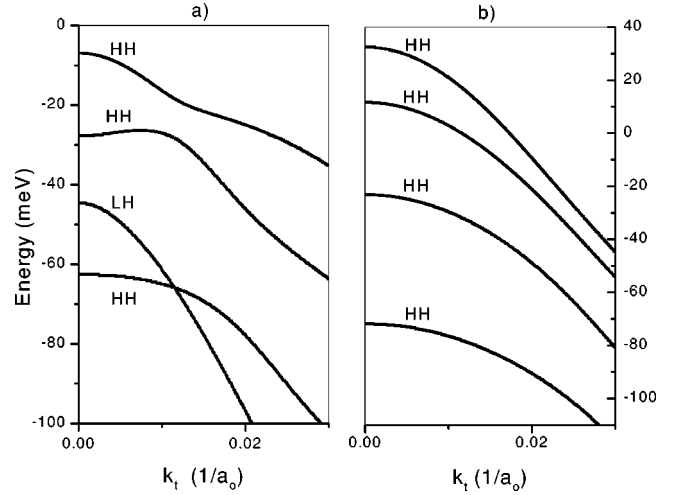


FIG. 1. The valence subbands used in the calculations: (a) Unstrained quantum well. (b) Quantum well under 2% compressive strain.

confused with the eigenvalue under space inversion; the operation σ is more useful here than space inversion because it keeps the value of \mathbf{k}_t unchanged. Since the time reversal and reflection operators anticommute—i.e., the time reversal operator changes the parity eigenvalue of a state—there exists an operator that changes the parity of the eigenfunction.¹¹ For any \mathbf{k}_t the system is at least doubly degenerate, and if one of the eigenfunction of a certain parity is found to be $[f_1(z), f_2(z), f_3(z), f_4(z)]^T e^{i(k_x x + k_y y)}$, the other (parity) degenerate eigenstate is given by $[f_4^*(z), f_3^*(z), f_2^*(z), f_1^*(z)]^T e^{i(k_x x + k_y y)}$.

B. Conduction subband

The conduction states in the quantum well are described by spinor wave functions of the form

$$\psi(\mathbf{r}) = \mu_{(S, \pm 1/2)}(\mathbf{r}) G(\mathbf{r}), \quad (4)$$

where

$$\mu_{(S, 1/2)}(\mathbf{r}) = S(\mathbf{r}) \alpha,$$

$$\mu_{(S, -1/2)}(\mathbf{r}) = S(\mathbf{r}) \beta,$$

and $S(\mathbf{r})$ is the conduction band-edge Bloch function. The energy eigenstates are determined by seeking solutions of the form $G(\mathbf{r}) = g(k_t, z) e^{i(k_x x + k_y y)}$ and solving the Schrödinger equation¹⁰ for the envelope function $g_n(z)$:

$$\left[-\frac{\hbar^2}{2m_c} \frac{d^2}{dz^2} + \frac{\hbar^2 k_t^2}{2m_c} + R_\epsilon \right] g_n(k_t, z) = E_n(k_t) g_n(k_t, z), \quad (5)$$

where m_c is the effective mass of the conduction electrons in the bulk structure. The effect of biaxial strain on the dispersion relation of the conduction subbands is described by the parameter $R_\epsilon = 2a_c[(c_{11} - c_{12})/c_{11}]\epsilon$. Since the quantum well is symmetric with respect to the center of the quantum well, the bound-state solutions of Eq. (5) are nondegenerate

(other than spin degeneracy) and alternate between even and odd (under $z \rightarrow -z$ transformation) states, always beginning with an even state.⁹ In the following calculations, we consider the optical properties of the 10-nm quantum well at photon energies up to 100 meV above the band edge; in this regime, only the first conduction subband needs to be considered.

C. Parameters and matrix elements

For both the valence and conduction subbands, then, we have at least a double degeneracy at each \mathbf{k}_t , and we label our spinor wave functions as $\psi_{n_s \mathbf{k}_t}(\mathbf{r})$, where n is a subband index and s a degeneracy index. Typically we use n or m if we refer to an arbitrary subband, with s or p as degeneracy indices; we retain c and v , respectively, to refer specifically to conduction and valence subbands. We discretize the \mathbf{k}_t , associated with an area \mathcal{A} in the xy plane; the wave functions are normalized when integrated over that area and over all z . Only at the very end of the calculation do we consider $\mathcal{A} \rightarrow \infty$ by taking $\mathcal{A}^{-1} \sum_{\mathbf{k}_t} \rightarrow \int d\mathbf{k}_t / (2\pi)^2$ in the usual way.

Using the wave functions described above, we calculate the velocity matrix elements $v_{n_s, m, p}^a(\mathbf{k}_t) = \langle n_s \mathbf{k}_t | v^a | m p \mathbf{k}_t \rangle$, spin matrix elements $S_{n_s, m, p}^a(\mathbf{k}_t) = \langle n_s \mathbf{k}_t | S^a | m p \mathbf{k}_t \rangle$, and spin-velocity matrix elements $K_{n_s, m, p}^{ab}(\mathbf{k}_t) = \langle n_s \mathbf{k}_t | v^a S^b | m p \mathbf{k}_t \rangle$ between different valence and conduction states of the quantum well; superscripts denote Cartesian components. Sometimes we use a single capital letter to denote both a band and degeneracy index, writing, e.g., $v_{NM}^a(\mathbf{k}_t)$ for $v_{n_s, m, p}^a(\mathbf{k}_t)$; we reserve C and V for conduction and valence bands, respectively. The first conduction subband and first four valence subbands shown in Fig. 1 are used as intermediate states in our calculations.

In the independent particle approximation adopted here, time reversal invariance leads to the following property of the matrix elements:¹⁴

$$v_{n_s, m, p}^{a*}(-\mathbf{k}_t) = -\exp(i\lambda_{nm}) v_{n_s, m, p}^a(\mathbf{k}_t),$$

$$S_{c, s, c, p}^{a*}(-\mathbf{k}_t) = -\exp(i\lambda'_{nm}) S_{c, s, c, p}^a(\mathbf{k}_t),$$

and

$$K_{c, s, c, p}^{ab*}(\mathbf{k}_t) = \exp(i\lambda''_{nm}) K_{c, s, c, p}^{ab}(-\mathbf{k}_t)$$

where \bar{s} designates the opposite degeneracy index of s and λ_{nm} , λ'_{nm} , and λ''_{nm} are arbitrary phases.

The matrix elements between the valence states were calculated using the general formalism proposed by Chang and James¹⁵ and Szmulowicz.¹⁶ The accuracy of the velocity matrix elements obtained was verified by calculating the diagonal (intrasubband) velocity matrix element, which was directly compared to the energy subband gradients. The matrix elements between conduction states were calculated using the envelope function.⁹ The material parameters used in our GaAs quantum well calculations are given in Table I.⁹

III. COHERENT CONTROL

Our calculations here follow earlier theoretical and experimental studies of the interference of quantum mechanical processes to control the direction of propagation of injection carriers in bulk semiconductors,^{5-7,17-22} and we refer to the literature for details of the experimental geometries and the general theoretical description. In contrast to coherent control of ionization from doped quantum wells,²³ we restrict ourselves here to injection within the plane of the quantum well and across the band gap. Recently Bhat and Sipe⁵ have shown that it is possible to coherently control spin currents injected in bulk semiconductors. For some experimental configurations the injected spin currents have an accompanying electrical current;²² one measure of the degree of spin polarization of the spin current in bulk indicates a polarization of 57%. One can also generate *pure* spin currents where a sorting of optically injected spins gives rise to electrons propagating in two opposite spatial directions with opposite average spins.^{6,7} The direction of the propagation of the injected currents can be controlled via the relative phase of the optical fields.²² While the underlying physics of the injection process in quantum well structures is the same as in bulk, the qualitative nature of these processes is significantly modified by the heterostructure geometry, as our calculations below demonstrate.

A. Injection process

Here we consider the scenario where a quantum well is subjected to two monochromatic optical fields of frequencies ω and 2ω . The unperturbed Hamiltonian in the independent-particle, second-quantized form is given by

$$H_o = \sum_{C\mathbf{k}_t} \hbar \omega_C(\mathbf{k}_t) a_{C\mathbf{k}_t}^\dagger a_{C\mathbf{k}_t} - \sum_{V\mathbf{k}_t} \hbar \omega_V(\mathbf{k}_t) b_{V\mathbf{k}_t}^\dagger b_{V\mathbf{k}_t},$$

and in the presence of an applied vector potential $\mathbf{A}(t)$ the interaction Hamiltonian is

$$H_{int}(t) = -\frac{e}{c} \mathbf{A}(t) \cdot \mathcal{V}(t),$$

where

$$\begin{aligned} \mathcal{V}(t) = & \sum_{CC'\mathbf{k}_t} a_{C\mathbf{k}_t}^\dagger a_{C'\mathbf{k}_t} \mathbf{v}_{CC'}(\mathbf{k}_t) e^{i\omega_{CC'}(\mathbf{k}_t)t} \\ & - \sum_{VV'\mathbf{k}_t} b_{V'\mathbf{k}_t}^\dagger b_{V\mathbf{k}_t} \mathbf{v}_{V'V}(\mathbf{k}_t) e^{i\omega_{V'V}(\mathbf{k}_t)t} \\ & + \sum_{CV\mathbf{k}_t} a_{C\mathbf{k}_t}^\dagger b_{V\mathbf{k}_t}^\dagger \mathbf{v}_{CV}(\mathbf{k}_t) e^{i\omega_{CV}(\mathbf{k}_t)t} \\ & + \sum_{CV\mathbf{k}_t} b_{V\mathbf{k}_t} a_{C\mathbf{k}_t} \mathbf{v}_{VC}(\mathbf{k}_t) e^{i\omega_{VC}(\mathbf{k}_t)t}. \end{aligned}$$

Here $a_{C\mathbf{k}_t}^\dagger$ ($a_{C\mathbf{k}_t}$) is the creation (annihilation) operator for an electron with conduction subband and spin indices denoted by C and $b_{V\mathbf{k}_t}^\dagger$ ($b_{V\mathbf{k}_t}$) is the corresponding creation (annihila-

tion) operator for a hole; $\hbar\omega_{C/V}(\mathbf{k}_t)$ is the energy of the conduction and valence subbands C/V at \mathbf{k}_t ; we have put $\omega_{NM}(\mathbf{k}_t) = \omega_N(\mathbf{k}_t) - \omega_M(\mathbf{k}_t)$. The vector potential describing the field is given by

$$\mathbf{A}(t) = \mathbf{A}(\omega)e^{-i(\omega+i\tau)t} + \mathbf{A}(-\omega)e^{i(\omega-i\tau)t} \\ + \mathbf{A}(2\omega)e^{-i(2\omega+i\tau)t} + \mathbf{A}(-2\omega)e^{i(2\omega-i\tau)t},$$

where τ is a small positive number that describes the turning on of the fields at $t = -\infty$; we set τ to zero at the end of the calculation. The electric field is related to the vector potential via $\mathbf{E}(\omega) = (i\omega/c)\mathbf{A}(\omega)$. Our treatment of the optical field approximates it as classical and assumes the long-wavelength (dipole approximation) limit. The optical field causes transitions from the ground state of the system $|0\rangle$ to the two-particle state $|CV\mathbf{k}_t\rangle \equiv a_{C\mathbf{k}_t}^\dagger b_{V\mathbf{k}_t}^\dagger |0\rangle$, where an electron from the valence subband and spin state V has been excited to the conduction subband and spin state C ; in the dipole approximation the two-dimensional crystal momentum vector is unchanged by the optical excitation. Adopting a perturbative approach, we write the state of the system at time t as

$$|\psi\rangle = C_o(t)|0\rangle + \sum_{C\mathbf{k}_t} C_{C\mathbf{k}_t}(t)|C\mathbf{k}_t\rangle$$

and determine the time evolution of the coefficient $C_{C\mathbf{k}_t}(t)$. Solving for $C_{C\mathbf{k}_t}(t)$ to second order in an electric field allows us to calculate the rate of change of the expectation value of any single-particle operator $\hat{\theta}$ using Fermi's golden rule:

$$\frac{d\langle\hat{\theta}\rangle}{dt} = \frac{d\langle\hat{\theta}\rangle_1}{dt} + \frac{d\langle\hat{\theta}\rangle_2}{dt} + \frac{d\langle\hat{\theta}\rangle_I}{dt}, \quad (6)$$

where $d\langle\hat{\theta}\rangle_1/dt$ describes the time evolution of the operator $\hat{\theta}$ due to one-photon (2ω) processes, $d\langle\hat{\theta}\rangle_2/dt$ that due to two-photon (ω) processes, and $d\langle\hat{\theta}\rangle_I/dt$ that due to the interference between excitations at frequencies ω and 2ω .

There are many interesting aspects of the subsequent relaxation of momentum²⁴ and spin¹ of the injected carriers. The spin relaxation time for a [001] GaAs quantum well is known to be a few picoseconds.²⁵ The momentum relaxation is expected to occur on a much shorter time scale and is due to many processes, such as phonon-carriers and carrier-carrier scattering. In the regime of high carrier density considered here, the latter is expected to dominate and be a major influence on the relaxation of both electrical and spin currents. As well, if an electrical current is present, the separation of the electrons and holes will lead to a space charge field that will also affect the transport of the injected carriers. This paper deals with the generation of electrical and spin currents in a quantum well; we defer the issue of relaxation to a later communication.

Each component of $d\langle\hat{\theta}\rangle/dt$ (6) will include contributions from the conduction subbands $d\langle\hat{\theta}\rangle^e/dt$ and valence subbands $d\langle\hat{\theta}\rangle^h/dt$:

$$\frac{d\langle\hat{\theta}\rangle}{dt} = \frac{d\langle\hat{\theta}\rangle^e}{dt} + \frac{d\langle\hat{\theta}\rangle^h}{dt},$$

$$\frac{d\langle\hat{\theta}\rangle^e}{dt} = 2\pi \sum_{C(C'),V,\mathbf{k}_t} \Omega_{C'V}^*(\mathbf{k}_t) \langle C'\mathbf{k}_t | \hat{\theta} | C\mathbf{k}_t \rangle \\ \times \Omega_{CV}(\mathbf{k}_t) \delta(2\omega - \omega_{CV}(\mathbf{k}_t)),$$

$$\frac{d\langle\hat{\theta}\rangle^h}{dt} = -2\pi \sum_{V(V'),C,\mathbf{k}_t} \Omega_{CV}(\mathbf{k}_t) \langle V\mathbf{k}_t | \hat{\theta} | V'\mathbf{k}_t \rangle \\ \times \Omega_{C'V'}^*(\mathbf{k}_t) \delta(2\omega - \omega_{CV}(\mathbf{k}_t)). \quad (7)$$

In the second of these equations our convention is $C = cs$, $C' = cs'$, etc.; that is, the states C and C' differ only by their spin index and hence $\omega_{CV}(\mathbf{k}_t) = \omega_{C'V}(\mathbf{k}_t)$. The notation $C(C'),V,\mathbf{k}_t$ indicates that the common subband index c and the two spin indices s and s' are to be summed over, as well as the valence bands their spin indices and transverse crystal momentum vectors \mathbf{k}_t . A similar convention is adopted in the third equation. Further,

$$\Omega_{CV}(\mathbf{k}_t) = \Omega_{CV}^I(\mathbf{k}_t) + \Omega_{CV}^{II}(\mathbf{k}_t),$$

$$\Omega_{CV}^I(\mathbf{k}_t) = \frac{ie}{\hbar} \frac{\mathbf{v}_{CV}(\mathbf{k}_t) \cdot \mathbf{E}(2\omega)}{2\omega},$$

$$\Omega_{CV}^{II}(\mathbf{k}_t) = -\left(\frac{e}{\hbar\omega}\right)^2 \sum_N \frac{[\mathbf{v}_{CN}(\mathbf{k}_t) \cdot \mathbf{E}(\omega)][\mathbf{v}_{NV}(\mathbf{k}_t) \cdot \mathbf{E}(\omega)]}{\omega_{CV}(\mathbf{k}_t)/2 + \omega_{VN}(\mathbf{k}_t)}, \quad (8)$$

where $\Omega_{CV}^I(\mathbf{k}_t)$ and $\Omega_{CV}^{II}(\mathbf{k}_t)$ correspond to the one- and two-photon transitions. Expanding these terms out, we have

$$\frac{d\langle\hat{\theta}\rangle^e}{dt} = \frac{d\langle\hat{\theta}\rangle_1^e}{dt} + \frac{d\langle\hat{\theta}\rangle_2^e}{dt} + \frac{d\langle\hat{\theta}\rangle_I^e}{dt},$$

$$\frac{d\langle\hat{\theta}\rangle_1^e}{dt} = 2\pi \sum_{C(C'),V,\mathbf{k}_t} \langle C'\mathbf{k}_t | \hat{\theta} | C\mathbf{k}_t \rangle \\ \times [\Omega_{CV}^I(\mathbf{k}_t) \Omega_{C'V}^{I*}(\mathbf{k}_t)] \delta(2\omega - \omega_{CV}(\mathbf{k}_t)),$$

$$\frac{d\langle\hat{\theta}\rangle_2^e}{dt} = 2\pi \sum_{C(C'),V,\mathbf{k}_t} \langle C'\mathbf{k}_t | \hat{\theta} | C\mathbf{k}_t \rangle \\ \times [\Omega_{CV}^{II}(\mathbf{k}_t) \Omega_{C'V}^{II*}(\mathbf{k}_t)] \delta(2\omega - \omega_{CV}(\mathbf{k}_t)),$$

$$\frac{d\langle\hat{\theta}\rangle_I^e}{dt} = 2\pi \sum_{C(C'),V,\mathbf{k}_t} \langle C'\mathbf{k}_t | \hat{\theta} | C\mathbf{k}_t \rangle \\ \times [\Omega_{CV}^I(\mathbf{k}_t) \Omega_{C'V}^{II*}(\mathbf{k}_t) + \text{c.c.}] \delta(2\omega - \omega_{CV}(\mathbf{k}_t)), \quad (9)$$

and similarly for the hole terms; the subscripts 1, 2, and I refer, respectively, to the one-photon contributions, two-photon contributions, and contribution due to the interference of amplitudes associated with those two processes. The quantities $\hat{\theta}$ of interest include the electrical and spin currents, and since the hole subbands generally have higher effective masses than the conduction subbands, the contributions made to the currents are dominated by the electronic contributions $d\langle\hat{\theta}\rangle^e/dt$. In the numerical calculations of this paper we focus on the contributions made by the conduction electrons, although the contributions from the holes can be similarly found.

B. Carrier and spin population

The operators for the areal carrier density \hat{n} and the a component \hat{S}^a of the spin areal density are given by

$$\hat{n} = \frac{1}{\mathcal{A}} \sum_{\mathbf{k}_t} \hat{n}(\mathbf{k}_t),$$

$$\hat{S}^a = \frac{1}{\mathcal{A}} \sum_{\mathbf{k}_t} \hat{S}^a(\mathbf{k}_t),$$

where

$$\hat{n}(\mathbf{k}_t) = \sum_C a_{C\mathbf{k}_t}^\dagger a_{C\mathbf{k}_t},$$

$$\hat{S}^a(\mathbf{k}_t) = \sum_{C(C')} S_{C'C}^a(\mathbf{k}_t) a_{C'\mathbf{k}_t}^\dagger a_{C\mathbf{k}_t}.$$

The population and spin injection rate into the quantum well then follow from the general form (6),

$$\frac{d\langle\hat{n}\rangle}{dt} = \frac{d\langle\hat{n}\rangle_1}{dt} + \frac{d\langle\hat{n}\rangle_2}{dt} + \frac{d\langle\hat{n}\rangle_I}{dt},$$

$$\frac{d\langle\hat{S}^a\rangle}{dt} = \frac{d\langle\hat{S}^a\rangle_1}{dt} + \frac{d\langle\hat{S}^a\rangle_2}{dt} + \frac{d\langle\hat{S}^a\rangle_I}{dt}.$$

We begin with the one-photon contributions. Using the term arising from $\Omega_{CV}^I(\mathbf{k}_t)$ alone in the second equation of Eqs. (7) [see the second equation of Eqs. (9)], the one-photon contribution to the carrier and spin population injection can be written as

$$\frac{d\langle\hat{n}\rangle_1}{dt} = \xi_1^{bc}(2\omega) E^{b*}(2\omega) E^c(2\omega),$$

$$\frac{d\langle\hat{S}^a\rangle_1}{dt} = \zeta_1^{abc}(2\omega) E^{b*}(2\omega) E^c(2\omega), \quad (10)$$

where the second-rank tensor $\xi_1^{bc}(2\omega) = \mathcal{A}^{-1} \sum_{\mathbf{k}_t} \xi_1^{bc}(2\omega; \mathbf{k}_t)$ and the third-rank pseudotensor $\zeta_1^{abc}(2\omega) = \mathcal{A}^{-1} \sum_{\mathbf{k}_t} \zeta_1^{abc}(2\omega; \mathbf{k}_t)$ are determined by

$$\xi_1^{bc}(2\omega; \mathbf{k}_t) = \frac{2\pi e^2}{\hbar^2} \sum_{C,V} \frac{v_{CV}^{b*}(\mathbf{k}_t) v_{CV}^c(\mathbf{k}_t)}{(2\omega)^2} \delta(2\omega - \omega_{CV}(\mathbf{k}_t)),$$

$$\zeta_1^{abc}(2\omega; \mathbf{k}_t) = \frac{2\pi e^2}{\hbar^2} \sum_{C(C'),V} \frac{S_{C'C}^a(\mathbf{k}_t) v_{C'V}^{b*}(\mathbf{k}_t) v_{CV}^c(\mathbf{k}_t)}{(2\omega)^2} \times \delta(2\omega - \omega_{CV}(\mathbf{k}_t)).$$

In all expressions involving tensors in this paper, summation over repeated indices is assumed. From the time reversal properties of the matrix elements (see discussion in Sec. II C) it can be shown that $\text{Re}[\xi_1^{bc}(2\omega; \mathbf{k}_t)]$ ($\text{Im}[\xi_1^{bc}(2\omega; \mathbf{k}_t)]$) and $\text{Im}[\zeta_1^{abc}(2\omega; \mathbf{k}_t)]$ ($\text{Re}[\zeta_1^{abc}(2\omega; \mathbf{k}_t)]$) are even (odd) under inversion in \mathbf{k}_t space ($\mathbf{k}_t \rightarrow -\mathbf{k}_t$). It follows from these properties that $\xi_1^{bc}(2\omega)$ is purely real and $\zeta_1^{abc}(2\omega)$ is purely imaginary, and that $\xi_1^{bc}(2\omega) = \xi_1^{cb}(2\omega)$ and $\zeta_1^{abc}(2\omega) = -\zeta_1^{acb}(2\omega)$, the latter holding necessarily since $\langle\hat{n}\rangle_1$ and $\langle\hat{S}^a\rangle_1$ are real.

Turning now to the two photon contributions, using the term arising from $\Omega_{CV}^{II}(\mathbf{k}_t)$ alone in the second equation of Eqs. (7) [see the third equation of Eqs. (9)], we find that the two-photon contribution to the carrier and spin population injection can be written as

$$\frac{d\langle\hat{n}\rangle_2}{dt} = \xi_2^{bcdf}(\omega) E^{b*}(\omega) E^{c*}(\omega) E^d(\omega) E^f(\omega),$$

$$\frac{d\langle\hat{S}^a\rangle_2}{dt} = \zeta_2^{abcdf}(\omega) E^{b*}(\omega) E^{c*}(\omega) E^d(\omega) E^f(\omega), \quad (11)$$

where the fourth-rank tensor $\xi_2^{bcdf}(\omega) = \mathcal{A}^{-1} \sum_{\mathbf{k}_t} \xi_2^{bcdf}(\omega; \mathbf{k}_t)$ and the fifth-rank pseudotensor $\zeta_2^{abcdf}(\omega) = \mathcal{A}^{-1} \sum_{\mathbf{k}_t} \zeta_2^{abcdf}(\omega; \mathbf{k}_t)$ are determined by

$$\xi_2^{bcdf}(\omega; \mathbf{k}_t) = \frac{2\pi e^4}{\hbar^4} \sum_{C,V,N,M} \frac{v_{CM}^{b*}(\mathbf{k}_t) v_{MV}^{c*}(\mathbf{k}_t) v_{CN}^d(\mathbf{k}_t) v_{NV}^f(\mathbf{k}_t)}{\omega^4 [\omega_{CV}(\mathbf{k}_t)/2 + \omega_{VN}(\mathbf{k}_t)] [\omega_{C'V}(\mathbf{k}_t)/2 + \omega_{VM}(\mathbf{k}_t)]} \delta(2\omega - \omega_{CV}(\mathbf{k}_t)),$$

$$\zeta_2^{abcdf}(\omega; \mathbf{k}_t) = \frac{2\pi e^4}{\hbar^4} \sum_{C(C'),V,N,M} \frac{S_{C'C}^a(\mathbf{k}_t) v_{C'M}^{b*}(\mathbf{k}_t) v_{MV}^{c*}(\mathbf{k}_t) v_{CN}^d(\mathbf{k}_t) v_{NV}^f(\mathbf{k}_t)}{\omega^4 [\omega_{CV}(\mathbf{k}_t)/2 + \omega_{VN}(\mathbf{k}_t)] [\omega_{C'V}(\mathbf{k}_t)/2 + \omega_{VM}(\mathbf{k}_t)]} \delta(2\omega - \omega_{CV}(\mathbf{k}_t)).$$

Since repeated Cartesian components in Eqs. (11) are to be summed over, with impunity we can symmetrize the expressions for $\xi_2^{bcdf}(\omega)$ and $\zeta_2^{abcdf}(\omega)$ with respect to interchanging b and c and with respect to interchanging d and f ; thus we do, although we do not write out those expressions explicitly. Again, using the time reversal properties of the matrix elements, we find that the susceptibility distributions $\text{Re}[\xi_2^{bcdf}(\omega, \mathbf{k}_t)]$ ($\text{Im}[\xi_2^{bcdf}(\omega, \mathbf{k}_t)]$) and $\text{Im}[\zeta_2^{abcdf}(\omega, \mathbf{k}_t)]$ ($\text{Re}[\zeta_2^{abcdf}(\omega, \mathbf{k}_t)]$) are even (odd) under inversion in \mathbf{k}_t space ($\mathbf{k}_t \rightarrow -\mathbf{k}_t$). It also follows that $\xi_2^{bcdf}(\omega)$ is purely real and $\zeta_2^{bcdf}(\omega)$ is purely imaginary, and that $\xi_2^{bcdf}(\omega) = \xi_2^{dfbc}(\omega)$ and $\zeta_2^{abcdf}(\omega) = -\zeta_2^{adfb}(\omega)$; the latter are required by the reality of $\langle \hat{n} \rangle_2$ and $\langle \hat{S}^a \rangle_2$.

Finally, we turn to the terms in the carrier and spin injection resulting from the interference of one- and two-photon absorption processes. These correspond to the last term in Eqs. (9). We find

$$\xi_I^{abcd}(\omega; \mathbf{k}_t) = -i \frac{\pi e^3}{\hbar^3} \sum_{C(C'), V, N} \frac{S_{C', C}^a(\mathbf{k}_t) v_{CN}^{b*}(\mathbf{k}_t) v_{NV}^{c*}(\mathbf{k}_t) v_{C', V}^d(\mathbf{k}_t)}{\omega^3 [\omega_{CV}(\mathbf{k}_t)/2 + \omega_{VN}(\mathbf{k}_t)]} \delta(2\omega - \omega_{CV}(\mathbf{k}_t)).$$

Using time reversal symmetry, it can be shown that $\text{Re}[\xi_I^{abcd}(\omega; \mathbf{k}_t)]$ ($\text{Im}[\xi_I^{abcd}(\omega; \mathbf{k}_t)]$) and $\text{Im}[\zeta_I^{abcd}(\omega; \mathbf{k}_t)]$ ($\text{Re}[\zeta_I^{abcd}(\omega; \mathbf{k}_t)]$) are even (odd), under inversion in \mathbf{k}_t space ($\mathbf{k}_t \rightarrow -\mathbf{k}_t$). These properties lead to purely real (imaginary) $\xi_I^{abcd}(\omega)$ ($\zeta_I^{abcd}(\omega)$) tensors.

If the inversion asymmetry in the underlying crystal is neglected, as we do here, then there is no contribution to the net carrier and spin injection rates, due to interference, $\xi_I^{abcd}(\omega) = \zeta_I^{abcd}(\omega) = 0$ (Ref. 26). Nonetheless, because at a given \mathbf{k}_t neither $\xi_I^{abcd}(\omega; \mathbf{k}_t)$ nor $\zeta_I^{abcd}(\omega; \mathbf{k}_t)$ will in general vanish, there will be interference contributions to both $d\langle \hat{n}(\mathbf{k}_t) \rangle/dt$ and $d\langle \hat{S}^a(\mathbf{k}_t) \rangle/dt$. Following the approach used above for the global expressions $d\langle \hat{n} \rangle/dt$ and $d\langle \hat{S}^a \rangle/dt$, we find immediately that

$$\begin{aligned} \frac{d\langle \hat{n}(\mathbf{k}_t) \rangle}{dt} &= \xi_1^{bc}(2\omega, \mathbf{k}_t) E^{b*}(2\omega) E^c(2\omega) \\ &+ \xi_2^{bcdf}(\omega, \mathbf{k}_t) E^{b*}(\omega) E^{c*}(\omega) E^d(\omega) E^f(\omega) \\ &+ 2\text{Re}[\xi_I^{abcd}(\omega, \mathbf{k}_t) E^{b*}(\omega) E^{c*}(\omega) E^d(2\omega)], \end{aligned}$$

$$\begin{aligned} \frac{d\langle \hat{S}^a(\mathbf{k}_t) \rangle}{dt} &= \zeta_1^{abc}(2\omega, \mathbf{k}_t) E^{b*}(2\omega) E^c(2\omega) \\ &+ \zeta_2^{abcdf}(\omega, \mathbf{k}_t) E^{b*}(\omega) E^{c*}(\omega) E^d(\omega) E^f(\omega) \\ &+ 2\text{Re}[\zeta_I^{abcd}(\omega, \mathbf{k}_t) E^{b*}(\omega) E^{c*}(\omega) E^d(2\omega)]. \end{aligned}$$

(13)

$$\frac{d\langle \hat{n} \rangle_I}{dt} = \xi_I^{bcd}(\omega) E^{b*}(\omega) E^{c*}(\omega) E^d(2\omega) + \text{c.c.},$$

$$\frac{d\langle \hat{S}^a \rangle_I}{dt} = \zeta_I^{abcd}(\omega) E^{b*}(\omega) E^{c*}(\omega) E^d(2\omega) + \text{c.c.}, \quad (12)$$

where the third-rank tensor $\xi_I^{abc}(\omega) = \mathcal{A}^{-1} \sum_{\mathbf{k}_t} \xi_I^{abc}(\omega; \mathbf{k}_t)$ and the fourth-rank pseudotensor $\zeta_I^{abcd}(\omega) = \mathcal{A}^{-1} \sum_{\mathbf{k}_t} \zeta_I^{abcd}(\omega; \mathbf{k}_t)$ are determined by

$$\begin{aligned} \xi_I^{bcd}(\omega; \mathbf{k}_t) &= -i \frac{\pi e^3}{\hbar^3} \sum_{C, V, N} \frac{v_{CN}^{b*}(\mathbf{k}_t) v_{NV}^{c*}(\mathbf{k}_t) v_{CV}^d(\mathbf{k}_t)}{\omega^3 [\omega_{CV}(\mathbf{k}_t)/2 + \omega_{VN}(\mathbf{k}_t)]} \\ &\times \delta(2\omega - \omega_{CV}(\mathbf{k}_t)), \end{aligned}$$

The third term in the above expression leads to a polar asymmetry in the \mathbf{k}_t -space distribution of the carrier and spin population. The asymmetry in the carrier population suggests a net electric current and that in the spin population a net spin current. These currents are the subject of the next section.

C. Electrical and spin currents

To calculate the currents injected in the quantum well we directly employ the areal electrical current density (\hat{J}^a) and areal spin current density ($\hat{K}^{ab} = \hat{v}^a \hat{S}^b$) operators

$$\hat{J}^a = \frac{1}{\mathcal{A}} \sum_{\mathbf{k}_t} \hat{J}^a(\mathbf{k}_t), \quad \hat{K}^{ab} = \frac{1}{\mathcal{A}} \sum_{\mathbf{k}_t} \hat{K}^{ab}(\mathbf{k}_t),$$

where

$$\hat{J}^a(\mathbf{k}_t) = e \sum_{C(C')} v_{CC'}^a(\mathbf{k}_t) a_{C', \mathbf{k}_t}^\dagger a_{C, \mathbf{k}_t},$$

$$\hat{K}^{ab}(\mathbf{k}_t) = \sum_{C(C')} K_{CC'}^{ab}(\mathbf{k}_t) a_{C', \mathbf{k}_t}^\dagger a_{C, \mathbf{k}_t},$$

to find from (6), using the approach employed above, that

$$\frac{d\langle \hat{J}^a \rangle}{dt} = \frac{d\langle \hat{J}^a \rangle_1}{dt} + \frac{d\langle \hat{J}^a \rangle_2}{dt} + \frac{d\langle \hat{J}^a \rangle_I}{dt},$$

$$\frac{d\langle \hat{K}^{ab} \rangle}{dt} = \frac{d\langle \hat{K}^{ab} \rangle_1}{dt} + \frac{d\langle \hat{K}^{ab} \rangle_2}{dt} + \frac{d\langle \hat{K}^{ab} \rangle_I}{dt},$$

where the one-photon terms are given by

$$\frac{d\langle \hat{J}^a \rangle_1}{dt} = \eta_1^{acd}(2\omega) E^{c*}(2\omega) E^d(2\omega),$$

$$\frac{d\langle \hat{K}^{ab} \rangle_1}{dt} = \mu_1^{abcd}(2\omega) E^{c*}(2\omega) E^d(2\omega),$$

with $\eta_1^{acd}(2\omega) = \mathcal{A}^{-1} \sum_{\mathbf{k}_t} \eta_1^{acd}(2\omega; \mathbf{k}_t)$, $\mu_1^{abcd}(2\omega) = \mathcal{A}^{-1} \sum_{\mathbf{k}_t} \mu_1^{abcd}(2\omega; \mathbf{k}_t)$, and

$$\eta_1^{acd}(2\omega; \mathbf{k}_t) = \frac{2\pi e^3}{\hbar^2} \sum_{C(C'), V} \frac{v_{C'C}^a(\mathbf{k}_t) v_{C'V}^{c*}(\mathbf{k}_t) v_{CV}^d(\mathbf{k}_t)}{(2\omega)^2} \times \delta(2\omega - \omega_{CV}(\mathbf{k}_t)),$$

$$\mu_1^{abcd}(2\omega; \mathbf{k}_t) = \frac{2\pi e^2}{\hbar^2} \sum_{C(C'), V} \frac{K_{C'C}^{ab}(\mathbf{k}_t) v_{C'V}^{c*}(\mathbf{k}_t) v_{CV}^d(\mathbf{k}_t)}{(2\omega)^2} \times \delta(2\omega - \omega_{CV}(\mathbf{k}_t)),$$

and the two-photon terms are given by

$$\frac{d\langle \hat{J}^a \rangle_2}{dt} = \eta_2^{acdfg}(2\omega) E^{c*}(\omega) E^{d*}(\omega) E^f(\omega) E^g(\omega),$$

$$\frac{d\langle \hat{K}^{ab} \rangle_2}{dt} = \mu_2^{abcdfg}(2\omega) E^{c*}(\omega) E^{d*}(\omega) E^f(\omega) E^g(\omega),$$

with $\eta_2^{acdfg}(\omega) = \mathcal{A}^{-1} \sum_{\mathbf{k}_t} \eta_2^{acdfg}(\omega; \mathbf{k}_t)$, $\mu_2^{abcdfg}(\omega) = \mathcal{A}^{-1} \sum_{\mathbf{k}_t} \mu_2^{abcdfg}(\omega; \mathbf{k}_t)$, and

$$\eta_2^{acdfg}(\omega; \mathbf{k}_t) = \frac{2\pi e^5}{\hbar^4} \sum_{C(C'), V, N, M} \frac{v_{C'C}^a(\mathbf{k}_t) v_{C'M}^{c*}(\mathbf{k}_t) v_{MV}^{d*}(\mathbf{k}_t) v_{CN}^f(\mathbf{k}_t) v_{NV}^g(\mathbf{k}_t)}{\omega^4 [\omega_{CV}(\mathbf{k}_t)/2 + \omega_{VN}(\mathbf{k}_t)] [\omega_{C'V}(\mathbf{k}_t)/2 + \omega_{VM}(\mathbf{k}_t)]} \delta(2\omega - \omega_{CV}(\mathbf{k}_t)),$$

$$\mu_2^{abcdfg}(\omega; \mathbf{k}_t) = \frac{2\pi e^4}{\hbar^4} \sum_{C(C'), V, N, M, \mathbf{k}_t} \frac{K_{C'C}^{ab}(\mathbf{k}_t) v_{C'M}^{c*}(\mathbf{k}_t) v_{MV}^{d*}(\mathbf{k}_t) v_{CN}^f(\mathbf{k}_t) v_{NV}^g(\mathbf{k}_t)}{\omega^4 [\omega_{CV}(\mathbf{k}_t)/2 + \omega_{VN}(\mathbf{k}_t)] [\omega_{C'V}(\mathbf{k}_t)/2 + \omega_{VM}(\mathbf{k}_t)]} \delta(2\omega - \omega_{CV}(\mathbf{k}_t)),$$

which can be symmetrized under the exchange of c with d and f with g . These one- and two-photon terms, when summed over the Brillouin zone to yield the net electrical current and spin current, vanish for models such as ours which neglect the lack of inversion symmetry of the crystal.²⁷ Thus the only currents that survive are due to the quantum mechanical interference between the one- and two-photon absorption processes; they take the form

$$\frac{d\langle \hat{J}^a \rangle_I}{dt} = \eta_I^{acdf}(\omega) E^{c*}(\omega) E^{d*}(\omega) E^f(2\omega) + \text{c.c.},$$

$$\frac{d\langle \hat{K}^{ab} \rangle_I}{dt} = \mu_I^{abcdf}(\omega) E^{c*}(\omega) E^{d*}(\omega) E^f(2\omega) + \text{c.c.}, \quad (14)$$

with $\eta_I^{acdf}(\omega) = \mathcal{A}^{-1} \sum_{\mathbf{k}_t} \eta_I^{acdf}(\omega; \mathbf{k}_t)$, $\mu_I^{abcdf}(\omega) = \mathcal{A}^{-1} \sum_{\mathbf{k}_t} \mu_I^{abcdf}(\omega; \mathbf{k}_t)$, and

$$\eta_I^{acdf}(\omega; \mathbf{k}_t) = -i \frac{\pi e^4}{\hbar^3} \sum_{C(C'), V, N} \frac{v_{CC'}^a(\mathbf{k}_t) v_{C'N}^{c*}(\mathbf{k}_t) v_{NV}^{d*}(\mathbf{k}_t) v_{CV}^f(\mathbf{k}_t)}{\omega_{CV}^3(\mathbf{k}_t) [\omega_{CV}(\mathbf{k}_t)/2 + \omega_{VN}(\mathbf{k}_t)]} \delta(2\omega - \omega_{CV}(\mathbf{k}_t)),$$

$$\mu_I^{abcdf}(\omega; \mathbf{k}_t) = -i \frac{\pi e^3}{\hbar^3} \sum_{C(C'), V, N} \frac{K_{CC'}^{ab}(\mathbf{k}_t) v_{C'N}^{c*}(\mathbf{k}_t) v_{NV}^{d*}(\mathbf{k}_t) v_{CV}^f(\mathbf{k}_t)}{\omega_{CV}^3(\mathbf{k}_t) [\omega_{CV}(\mathbf{k}_t)/2 + \omega_{VN}(\mathbf{k}_t)]} \delta(2\omega - \omega_{CV}(\mathbf{k}_t)).$$

The fourth-rank tensor $\eta_I^{acdf}(\omega)$ and fifth-rank pseudotensor $\mu_I^{abcdf}(\omega)$ can be symmetrized under the exchange of c and d , although we do not explicitly write out those expressions here. From the time reversal properties of the matrix elements it follows that $\eta_I^{acdf}(\omega)$ is purely imaginary and $\mu_I^{abcdf}(\omega)$ is purely real.

In the same way that we could characterize the carrier and spin injection in the last section by $d\langle \hat{n}(\mathbf{k}_t) \rangle/dt$ and $d\langle \hat{S}^a(\mathbf{k}_t) \rangle/dt$, we can here study the current density and spin

current density throughout the Brillouin zone by the corresponding quantities $d\langle \hat{J}^a(\mathbf{k}_t) \rangle/dt$ and $d\langle \hat{K}^{ab}(\mathbf{k}_t) \rangle/dt$,

$$\begin{aligned} \frac{d\langle \hat{J}^a(\mathbf{k}_t) \rangle}{dt} &= \eta_1^{acd}(2\omega, \mathbf{k}_t) E^{c*}(2\omega) E^d(2\omega) \\ &+ \eta_2^{acdfg}(\omega, \mathbf{k}_t) E^{c*}(\omega) E^{d*}(\omega) E^f(\omega) E^g(\omega) \\ &+ 2\text{Re}[\eta_I^{acdf}(\omega, \mathbf{k}_t) E^{c*}(\omega) E^{d*}(\omega) E^f(2\omega)], \end{aligned}$$

$$\begin{aligned} \frac{d\langle \widehat{K}^{ab}(\mathbf{k}_t) \rangle}{dt} &= \mu_1^{abcd}(2\omega, \mathbf{k}_t) E^{c*}(2\omega) E^d(2\omega) \\ &+ \mu_2^{abcdfg}(\omega, \mathbf{k}_t) E^{c*}(\omega) E^{d*}(\omega) E^f(\omega) E^g(\omega) \\ &+ 2\text{Re}[\mu_I^{abcdf}(\omega, \mathbf{k}_t) E^{c*}(\omega) E^{d*}(\omega) E^f(2\omega)]. \end{aligned}$$

Injection of spin-polarized currents due to one-photon absorption in semiconductor wells has been reported.²⁸ The currents discussed here are different, because, among other reasons, the effects presented here do not rely on a lack of inversion symmetry of the crystal and the presence of ω and 2ω optical fields here allows the use of the phases of the fields as control parameters.

D. Consequences of symmetry

A [001] GaAs (zinc-blende) quantum well under (001) biaxial strain is invariant under the D_{2d} point group.²⁹ The point group symmetries can be used to reduce the number of independent and nonzero elements of all the tensor and pseudotensors discussed above. Some of the nonzero tensor and pseudotensor components allowed by symmetry describe currents and spin currents associated with carrier motion along the growth axis of the quantum well. In the infinite barrier model for the quantum well we adopt here these currents and spin currents vanish, and so we do not mention them further below; we plan to turn to them in future communication that will report calculations of these terms within a finite barrier model.

The fourth-rank tensors η_I^{acdf} that describe electrical currents (14) have 21 nonzero and 8 independent tensor components. The tensor components contributing to the injection of electrical current in the plane of the quantum well are

$$\begin{aligned} \eta^{xxxx} &= \eta^{yyyy}, \\ \eta^{xyyx} &= \eta^{yxyx}, \\ \eta^{xxyy} &= \eta^{yyxx} = \eta^{xyxy} = \eta^{yxyx}, \\ \eta^{xzzx} &= \eta^{yzzz}, \\ \eta^{xkzz} &= \eta^{yzzk} = \eta^{kzxx} = \eta^{kzyz}. \end{aligned}$$

The fifth-rank pseudotensors that describe spin currents (14) have 58 nonzero and 19 independent tensor components. The tensor components that contribute to the spin currents in the plane of the quantum well are

$$\begin{aligned} \mu^{xzxy} &= -\mu^{yzyx}, \\ \mu^{xzxy} &= \mu^{xzyx} = -\mu^{yzyx} = -\mu^{yzxy}, \\ \mu^{xzyy} &= -\mu^{yzxx}, \\ \mu^{xzzz} &= -\mu^{yzzx}, \\ \mu^{xzyz} &= \mu^{xzyz} = -\mu^{yzzz} = -\mu^{yzxz}, \\ \mu^{xxyx} &= \mu^{xyxz} = -\mu^{yyxz} = -\mu^{yyxy}, \\ \mu^{xxyx} &= \mu^{xxyx} = -\mu^{yyxz} = -\mu^{yyxy}, \\ \mu^{xzyx} &= \mu^{xyzx} = -\mu^{yyzx} = -\mu^{yyzy}, \\ \mu^{xyxz} &= -\mu^{xyyz}, \\ \mu^{xyxz} &= \mu^{xyzx} = -\mu^{xyzy} = -\mu^{yxzy}, \\ \mu^{xyyz} &= -\mu^{yxxz}, \\ \mu^{xyzy} &= \mu^{xyzx} = -\mu^{yxzy} = -\mu^{yxzy}, \\ \mu^{xyyz} &= -\mu^{yxxz}, \\ \mu^{xyzy} &= \mu^{xyzx} = -\mu^{yxzy} = -\mu^{yxzy}, \\ \mu^{xyzz} &= -\mu^{yxzz}. \end{aligned}$$

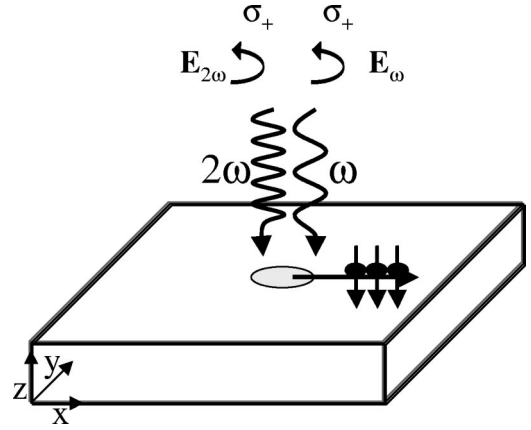


FIG. 2. Schematic illustration of cocircularly polarized optical fields propagating along the growth axis of the quantum well. A net spin-polarized electrical current is injected in the plane of the quantum well with average spin pointing along the growth axis of the quantum well.

IV. RESULTS: COHERENT CONTROL OF ELECTRICAL AND SPIN CURRENTS

We now look at the currents and spin currents that can be injected in the plane of the quantum well in a number of different experimental geometries. Throughout this section we take $E(\omega)$ and $E(2\omega)$ to be the real amplitudes of the beams at ω and 2ω , respectively, explicitly indicating the phase through unit polarization vectors $\hat{\mathbf{e}}_{\omega}$ and $\hat{\mathbf{e}}_{2\omega}$ such that $\hat{\mathbf{e}}_{\kappa} \cdot \hat{\mathbf{e}}_{\kappa}^* = 1$ for $\kappa = \omega$ or 2ω . Thus we generally write $\mathbf{E}_{\kappa} = E_{\kappa} \hat{\mathbf{e}}_{\kappa}$.

A. Two circularly polarized fields

As shown in Fig. 2, in this configuration the ω and 2ω optical fields are circularly polarized and are propagating along the quantum well growth axis. The electric fields of the propagating light beams are given by

$$\mathbf{E}(\omega) = E(\omega) e^{i\phi_{\omega}} \frac{(\hat{\mathbf{x}} + \alpha_{\omega} i \hat{\mathbf{y}})}{\sqrt{2}},$$

$$\mathbf{E}(2\omega) = E(2\omega) e^{i\phi_{2\omega}} \frac{(\hat{\mathbf{x}} + \alpha_{2\omega} i \hat{\mathbf{y}})}{\sqrt{2}},$$

where $\alpha_{\omega/2\omega} = \pm 1$. The currents injected into the quantum well are due to interference of the ω and 2ω photon excitations. The electrical current density arising from the interference of the ω and 2ω fields is expressed using the purely imaginary tensor η_I^{acdf} , Eqs. (14), and is given by

$$\begin{aligned} \frac{d\langle \mathbf{J} \rangle}{dt} &= [\text{Im}(\eta_I^{xxxx}) - \text{Im}(\eta_I^{xyyx}) \\ &+ 2\alpha_{\omega} \alpha_{2\omega} \text{Im}(\eta_I^{xyxy})] \frac{E(\omega)^2 E(2\omega)}{\sqrt{2}} \hat{\mathbf{m}}. \end{aligned} \quad (15)$$

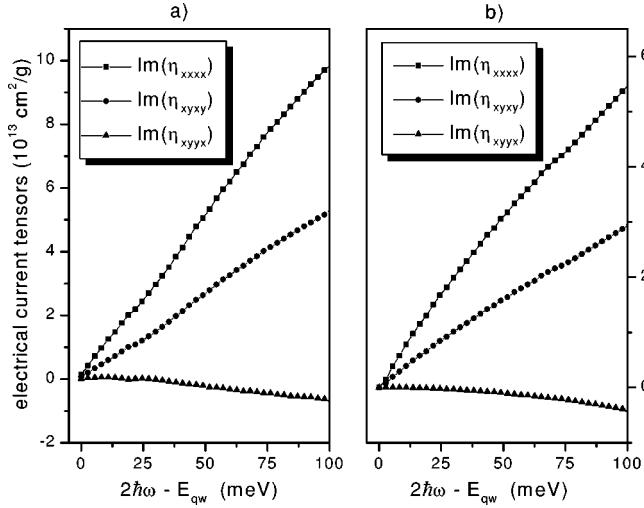


FIG. 3. The imaginary tensors η_I^{acdf} that relate to the electrical current, (a) unstrained quantum well, (b) quantum well with 2% biaxial compressive strain as a function of the photon energy of the 2ω beam relative to the band gap energy E_{qw} (E_{qw} is about 1.58 (1.7) eV for the unstrained (strained) quantum wells). The tensors shown, satisfy the condition $\eta_I^{xxxx} = 2\eta_I^{xyxy} + \eta_I^{xyyx}$, which holds for the isotropic case.

The imaginary parts of the tensor components η_I^{acdf} involved in the electrical current injection (15) are plotted in Fig. 3. The direction of injection $\hat{\mathbf{m}} = \sin(2\phi_\omega - \phi_{2\omega})\hat{\mathbf{x}} + \alpha_{2\omega} \cos(2\phi_\omega - \phi_{2\omega})\hat{\mathbf{y}}$ in the plane of the quantum well can be coherently controlled using the relative phase of the optical beams $2\phi_\omega - \phi_{2\omega}$. The injected electrical current is spin polarized with average spin pointing along the z direction and is described by the following nonzero components of the expectation value of the spin current density (14):

$$\begin{aligned} \frac{d\langle K^{xz} \rangle}{dt} &= -\alpha_{2\omega} [-\mu_I^{xzxy} + \mu_I^{xzyy} + 2\alpha_{2\omega}\alpha_\omega \mu_I^{xzyx}] \\ &\quad \times \frac{E(\omega)^2 E(2\omega)}{\sqrt{2}} \sin(2\phi_\omega - \phi_{2\omega}), \\ \frac{d\langle K^{yz} \rangle}{dt} &= [-\mu_I^{xzxy} + \mu_I^{xzyy} + 2\alpha_{2\omega}\alpha_\omega \mu_I^{xzyx}] \\ &\quad \times \frac{E(\omega)^2 E(2\omega)}{\sqrt{2}} \cos(2\phi_\omega - \phi_{2\omega}). \end{aligned} \quad (16)$$

The relevant real pseudotensor components μ_I^{abcd} are shown in Fig. 4.

Many of the parameters that characterize the injected quantities we study depend on the field intensities only through their dependence on a relative intensity parameter $\Xi \equiv I_\omega^2/I_{2\omega}$, where the intensity of the beams are specified by $I_{\omega/2\omega} = cE(\omega/2\omega)^2/(2\pi)$. For example, consider the average, or *swarm*, velocity of the injected carriers,

$$\mathbf{v}_{swarm} \equiv \frac{d\langle \mathbf{J} \rangle / dt}{e d\langle n \rangle / dt}.$$

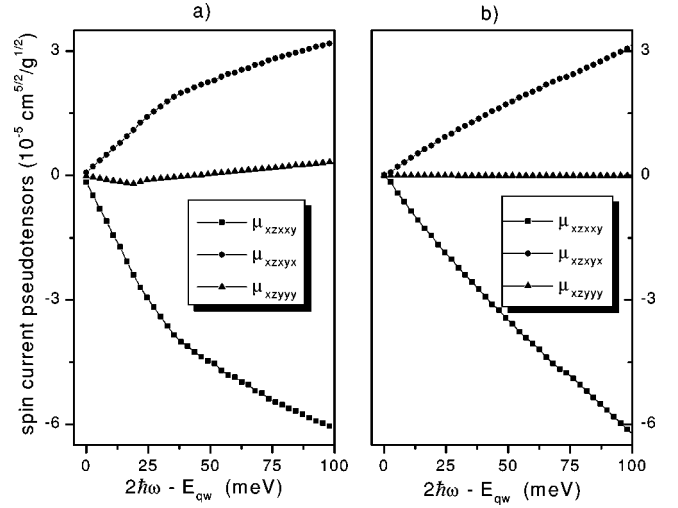


FIG. 4. The real pseudotensors μ_I^{abcd} that relate to the spin currents, (a) unstrained quantum well, (b) quantum well with 2% biaxial compressive strain as a function of the photon energy $2\hbar\omega$ relative to the band gap energy E_{qw} . The pseudotensors shown satisfy the condition $\mu_I^{xzxy} = -2\mu_I^{xzyx} + \mu_I^{xzyy}$, which holds in the isotropic limit.

For given polarization vectors \mathbf{e}_ω and $\mathbf{e}_{2\omega}$ this quantity has components

$$v_{swarm}^a = \frac{A\sqrt{\Xi}}{B + C\Xi},$$

where

$$\begin{aligned} A &= 2\sqrt{\frac{2\pi}{c}} i \eta_I^{abcd}(2\omega) \text{Im}(e_\omega^{b*} e_\omega^{c*} e_{2\omega}^d), \\ B &= \xi_1^{ab}(\omega) e_{2\omega}^{a*} e_{2\omega}^b, \\ C &= \frac{2\pi}{c} \xi_2^{abcd}(\omega) e_\omega^{a*} e_\omega^{b*} e_\omega^c e_\omega^d. \end{aligned}$$

The swarm velocity has a maximum value of $A/(2\sqrt{BC})$ at $\Xi = (B/C)$, when the one- and two-photon carrier population injections are equal. We consider cocircularly polarized optical fields—i.e., $\alpha_\omega = \alpha_{2\omega} = 1$ —and choose the relative phase of the optical fields such that a spin-polarized current is injected in the x direction; in Fig. 5, we plot the relative intensity parameter Ξ at which the swarm velocity is maximized and that maximum value. To characterize the spin polarization of the current we define a quantity $\bar{S}^z(\phi)$ in the following way. At a given 2ω the terms $d\langle \hat{\mathcal{J}}^a(\mathbf{k}_i) \rangle / dt$ and $d\langle \hat{\mathcal{K}}^{ab}(\mathbf{k}_i) \rangle / dt$ will survive at a set of \mathbf{k}_i^0 identified by the Dirac delta function $\delta(2\omega - \omega_{CV}(\mathbf{k}_i^0))$. For each \mathbf{k}_i^0 so defined that makes an angle ϕ from the $+x$ axis, increasing towards the $+y$ axis we evaluate³⁰

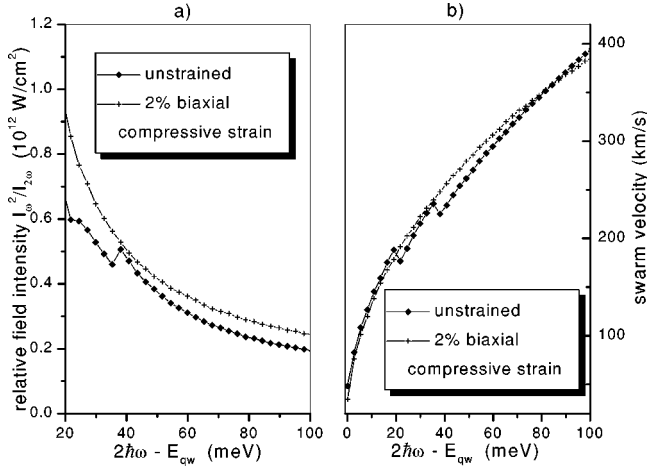


FIG. 5. (a) The relative intensity parameter $\Xi \equiv I_\omega^2/I_{2\omega}$ as a function of photon energy (relative to the band edge E_{qw}), which leads to the swarm velocity for the unstrained and 2% biaxially compressed quantum wells. (b) Swarm velocity of the injected carriers for the unstrained and 2% biaxially compressed quantum well.

$$\bar{S}^z(\phi) \equiv \frac{e \sum_{\mathbf{k}_i^0 \text{ at } \phi} [d\langle \hat{K}^{xz}(\mathbf{k}_i^0) \rangle / dt]}{\sum_{\mathbf{k}_i^0 \text{ at } \phi} [d\langle \hat{J}^z(\mathbf{k}_i^0) \rangle / dt]}. \quad (17)$$

A measure of the average spin polarization of the current is then given by

$$M_{avg} = \frac{1}{2\pi} \int_0^{2\pi} d\phi \bar{S}^z(\phi).$$

We plot this in Fig. 6 as a function of the photon energy of the 2ω optical field, at each photon energy for the relative intensity parameter Ξ that maximizes the swarm velocity.

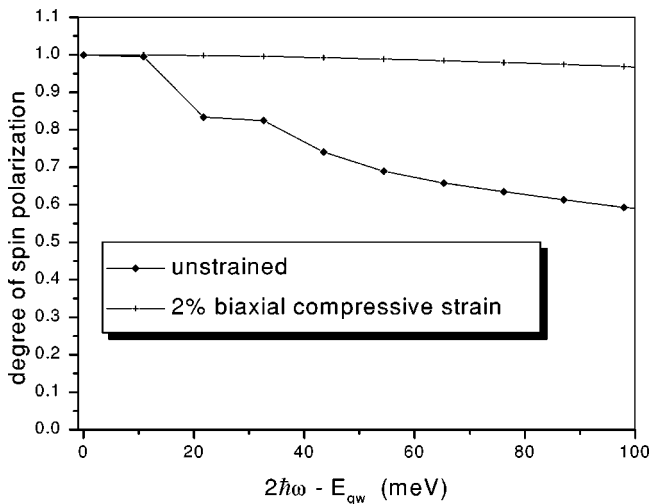


FIG. 6. Degree of spin polarization (in units of $\hbar/2$) of the injected carriers in the plane of an unstrained and 2% biaxially compressed quantum well as a function of the photon energy $2\hbar\omega$ relative to the band gap energy E_{qw} .

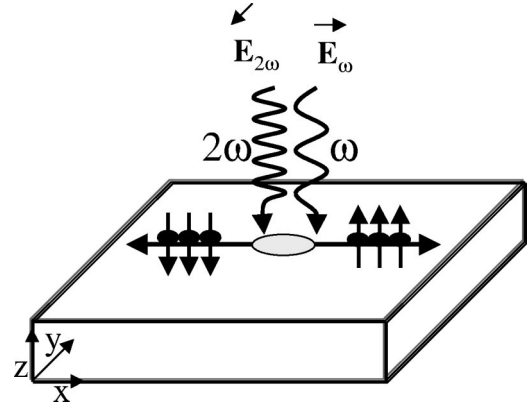


FIG. 7. Schematic illustration of cross-linearly polarized optical fields propagating along the growth axis of the quantum well. A pure spin current is injected in the plane of the quantum well when $\cos(2\phi_\omega - \phi_{2\omega}) \neq 0$.

For photon energies close to the band gap, the injected electrons are nearly 100% spin polarized, and as the light-hole-like subbands start to contribute to the injection, the degree of spin polarization drops to about 60% (Fig. 6). If the quantum well is compressively strained, the strain rearranges the valence subbands (Fig. 1) such that the light-hole subband starts contributing to the injection at a much higher photon energy; therefore a high degree of spin polarization of the injected current is maintained for excitations well above the band gap. The structure and trends that are present in Figs. 5(a) and 5(b) can be understood by looking at contributions made to the calculated quantities from the different subbands of Fig. 1. The relative intensity Ξ [Fig. 5(a)] that maximizes the swarm velocity diverges for photon energies at the band gap; this corresponds to injecting carriers at the bottom of the parabolic conduction subband, which would produce no average velocity.³¹ For the strained quantum well, from Figs. 5(b) and 6, it is clear that one can inject highly spin-polarized electrons with average velocity of a few hundreds of km/s.

B. Cross-linearly polarized optical fields

Figure 7 shows a configuration where the ω and 2ω beams are cross-linearly polarized, with the ω field polarized along the x and the 2ω beam polarized along the y direction, Eqs. (18). An electrical current can be injected along the y direction Eq. (19), and is proportional to a sinusoidal function of the relative phase of the two fields $2\phi_\omega - \phi_{2\omega}$:

$$\mathbf{E}(\omega) = E(\omega) e^{i\phi_\omega} \hat{\mathbf{x}},$$

$$\mathbf{E}(2\omega) = E(2\omega) e^{i\phi_{2\omega}} \hat{\mathbf{y}}, \quad (18)$$

$$\frac{d\langle \mathbf{J} \rangle}{dt} = 2\text{Im}(\eta_i^{xyxy}) E(\omega)^2 E(2\omega) \sin(2\phi_\omega - \phi_{2\omega}) \hat{\mathbf{y}}. \quad (19)$$

There is also a *pure* spin current in the plane of the quantum well,

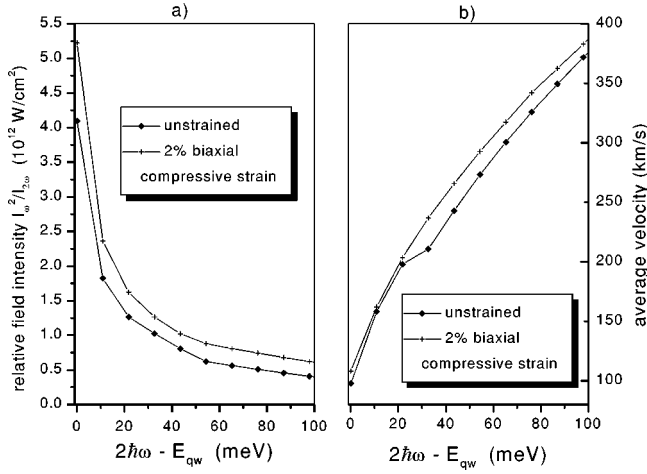


FIG. 8. (a) The relative intensity parameter $\Xi \equiv I_{\omega}^2/I_{2\omega}$ as a function of photon energy (relative to the band edge E_{qw}), which leads to the maximum spin polarization of the injected carriers in the unstrained and 2% biaxially compressed quantum wells. (b) Average velocity of the injected carriers for the unstrained and 2% biaxially compressed quantum well.

$$\frac{d\langle K^{xz} \rangle}{dt} = 2\mu_I^{xz,xyx} E(\omega)^2 E(2\omega) \cos(\phi_{2\omega} - 2\phi_{\omega}), \quad (20)$$

a spin current injected along the x direction with average spin pointing along the growth axis. No net electrical current exists in the x direction, but instead the translational motion of the injected electrons is correlated with their spin, electrons with a positive z component of spin going in one of the $\pm x$ directions, and those with a negative z component of spin in the other. This pure spin current has been experimentally observed.^{6,7} We focus on the pure spin current (\dot{K}^{xz} by choosing the relative phase of the fields such that $\dot{\mathbf{J}}=0$, Eq. (19), and \dot{K}^{xz} , Eq. (20), is maximized. Since there is no spin population injection due to one- and two-photon absorptions, the interference between the ω and 2ω excitations gives rise to an *odd* (under $\mathbf{k}_i \rightarrow -\mathbf{k}_i$) spin population injection distribution in \mathbf{k}_i space, which clearly corresponds to opposite average spin of the oppositely injected carriers. The susceptibilities $\eta_I^{xy,xy}$ and $\mu_I^{xz,xyx}$ that describe the electrical and spin currents are presented in Figs. 3 and 4.

The integral over ϕ of $\bar{S}^z(\phi)$, Eq. (17), vanishes here, but we can characterize the spin polarization of the pure spin current by the parameter

$$M_{pol}^z = \frac{1}{\pi} \int_{-\pi/2}^{\pi/2} [\bar{S}^z(\phi) - \bar{S}^z(\phi - \pi)] d\phi. \quad (21)$$

The relative intensity parameter Ξ that leads to maximum degree of spin polarization M_{pol}^z , Eq. (21), is shown in Fig. 8. The degrees of spin polarization M_{pol}^z , Eq. (21), of the injected spin current for the unstrained and 2% compressively strained quantum wells are shown in Fig. 9 at the value of the relative intensity parameter that maximizes it.

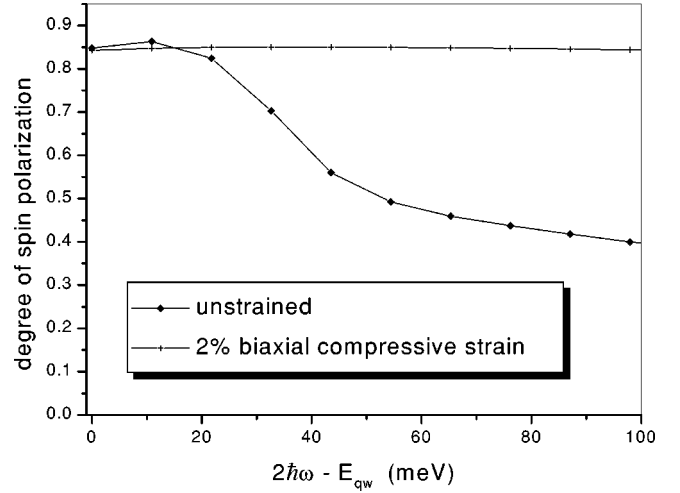


FIG. 9. Degree of spin polarization (in units of $\hbar/2$) of the pure spin current injected in the plane of an unstrained and 2% biaxially compressed quantum well as a function of the photon energy $2\hbar\omega$ relative to the band gap energy E_{qw} .

To characterize the velocity of the injected carriers we introduce a characteristic velocity $\bar{v}^x(\phi)$ along the lines used above for spin,

$$\bar{v}^x(\phi) \equiv \frac{\sum_{\mathbf{k}_i^0 \text{ at } \phi} d\langle \hat{\mathcal{F}}^x(\mathbf{k}_i^0) \rangle / dt}{e \sum_{\mathbf{k}_i^0 \text{ at } \phi} [d\langle \hat{n}(\mathbf{k}_i) \rangle / dt]}.$$

For this excitation geometry the integral of $\bar{v}^x(\phi)$ over all ϕ vanishes, but we can get a measure of the characteristic x component of the velocity of injected electrons by evaluating

$$v_{char}^x = \frac{1}{\pi} \int_{-\pi/2}^{\pi/2} \bar{v}^x(\phi) d\phi. \quad (22)$$

Figure 8 shows this characteristic velocity (22) of the injected electrons.

From Fig. 9, it is clear that for photon energies close to the band gap, the injected pure spin current is highly spin polarized with a degree of spin polarization of about 85%; as the light-hole-like subbands start to contribute to the injection, the degree of spin polarization of the pure spin currents reduces to about 35%. If the quantum well is compressively strained, a high degree of spin polarization of the injected pure spin current is maintained for excitations well above the gap. Once again, from Fig. 8(b) it is clear that the injected ballistic electrons can have an average velocity of a few hundreds of km/s, and this velocity decreases as photon energy reaches the band gap value. The absolute values of average velocity (22) and spin polarization (21) of the right- and left-moving electrons (along the direction of injection) are calculated to be identical.

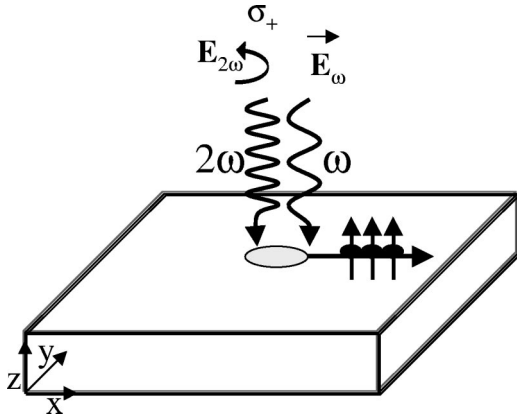


FIG. 10. Schematic illustration of circularly polarized $\mathbf{E}(2\omega)$ and linearly polarized $\mathbf{E}(\omega)$ optical fields propagating along the growth axis of the quantum well. A spin-polarized electrical current is injected in the plane of the quantum well.

C. 2ω is circularly polarized and ω is linearly polarized

In this section the configuration shown in Fig. 10 will be discussed. The 2ω beam which induces one-photon transitions is circularly polarized and the ω beam which is responsible for two-photon transitions is linearly polarized along the x direction Eqs. (23):

$$\begin{aligned} \mathbf{E}(\omega) &= E(\omega) e^{i\phi_{\omega}} \hat{\mathbf{x}}, \\ \mathbf{E}(2\omega) &= E(2\omega) e^{i\phi_{2\omega}} \frac{(\hat{\mathbf{x}} + \alpha_{2\omega} i \hat{\mathbf{y}})}{\sqrt{2}}, \end{aligned} \quad (23)$$

where $\alpha_{2\omega} = \pm 1$. A spin-polarized electrical current is injected in the plane of the quantum well. It is important to note that since the ω field is polarized along the x direction, there is an asymmetry in the plane of the quantum well with respect to the x and y axes. That is, the injected currents have different characteristics depending on whether the relative phase parameter $2\phi_{\omega} - \phi_{2\omega}$ is chosen such that the current is injected in the x or y direction. The injected electrical current density is described by

$$\frac{d\langle J^x \rangle}{dt} = \sqrt{2} \text{Im}(\eta_I^{xxxx}) E(\omega)^2 E(2\omega) \sin(2\phi_{\omega} - \phi_{2\omega}),$$

$$\frac{d\langle J^y \rangle}{dt} = -\alpha_{2\omega} \sqrt{2} \text{Im}(\eta_I^{xyxy}) E(\omega)^2 E(2\omega) \cos(2\phi_{\omega} - \phi_{2\omega}),$$

while the injected spin current density is described by

$$\frac{d\langle K^{xz} \rangle}{dt} = \sqrt{2} \alpha_{2\omega} \mu_I^{xzyx} E(\omega)^2 E(2\omega) \sin(2\phi_{\omega} - \phi_{2\omega}),$$

$$\frac{d\langle K^{yz} \rangle}{dt} = -\sqrt{2} \mu_I^{xzyy} E(\omega)^2 E(2\omega) \cos(2\phi_{\omega} - \phi_{2\omega}).$$

From Figs. 3 and 4, it is clear that for both the unstrained and strained quantum wells, $|\eta_I^{xxxx}(\omega)| \gg |\eta_I^{xyxy}(\omega)|$ and $|\mu_I^{xzyx}(\omega)| \gg |\mu_I^{xzyy}(\omega)|$. Therefore the net electrical and

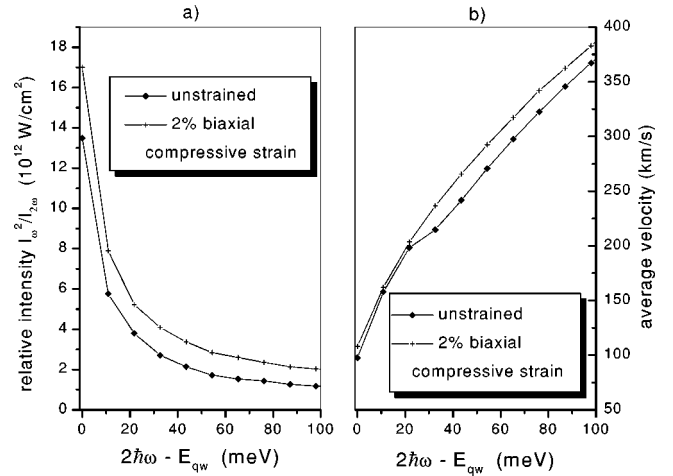


FIG. 11. (a) The relative intensity parameter $\Xi \equiv I_{\omega}^2 / I_{2\omega}$ as a function of photon energy (relative to the band edge E_{qw}), which leads to the maximum spin polarization of the injected carriers in the unstrained and 2% biaxially compressed quantum wells. (b) Average velocity of the injected carriers for the unstrained and 2% biaxially compressed quantum well.

spin currents are larger when the spin-polarized electrons are injected in the x direction; this current is maximized when the relative phase parameter satisfies $\cos(2\phi_{\omega} - \phi_{2\omega}) = 0$. In our calculations we use $\alpha_{2\omega} = 1$.

From examination of the injection of spin and carriers in \mathbf{k}_t space, Eqs. (13), it is found that the injected electrons in opposite directions have opposite average spin (pointing along the growth axis). We use Eqs. (21) and (22) to characterize the degree of spin polarization, M_{pol}^z , and average velocity v_{char}^x of the injected carriers. Figure 11 shows the relative intensity parameter $\Xi \equiv I_{\omega}^2 / I_{2\omega}$ that maximizes the spin polarization of the carriers. The corresponding average velocity of the injected carriers for the unstrained and 2% biaxially compressed quantum well is shown in Fig. 11. The maximized degree of spin polarization of the carriers is shown in Fig. 12.

Once again, for photon energies close to the band gap, the injected electrons are spin polarized. But the degree of spin polarization is only about 55%, and it falls to about 30% as the photon energy is increased. In the case of compressively strained quantum well the degree of spin polarization of the injected current is maintained for excitation energies well above the gap. For both the unstrained and strained quantum wells, the injected ballistic electrons can have an average velocity of a few hundreds of km/s [Fig. 11(b)].

D. Other possible experimental configurations

There are numerous other experimental configurations that can be used to inject electrical or spin currents with different properties. Here we only mention a few.

In the configuration where the ω field is circularly polarized $\mathbf{E}(\omega) = E(\omega) e^{i\phi_{\omega}} (\hat{\mathbf{x}} + \alpha_{\omega} i \hat{\mathbf{y}}) / \sqrt{2}$ and the 2ω field is linearly polarized $\mathbf{E}(2\omega) = E(2\omega) e^{i\phi_{2\omega}} \hat{\mathbf{x}}$, a spin-polarized electrical current is injected in the plane of the quantum well.

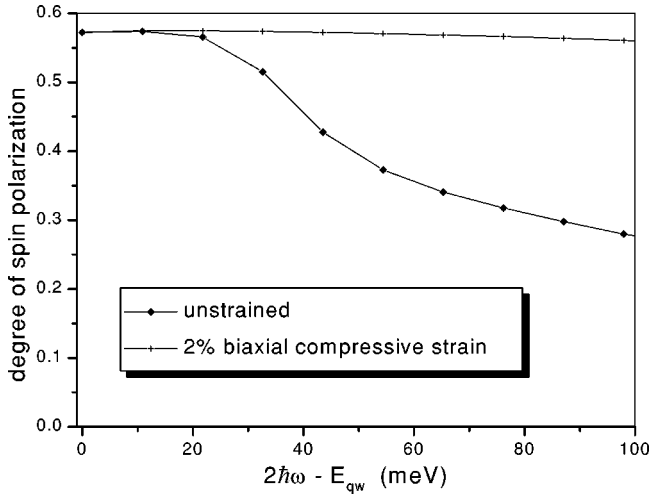


FIG. 12. Degree of spin polarization (in units of $\hbar/2$) of the injected carriers in the plane of an unstrained and 2% biaxially compressed quantum well as a function of the photon energy $2\hbar\omega$ relative to the band gap energy E_{qw} .

The current injected along x is described $J^x = \{\text{Im}(\eta_I^{xxxx}) - \text{Im}(\eta_I^{xyyx})\}E(\omega)^2E(2\omega) \sin(2\phi_\omega - \phi_{2\omega})$ with its spin polarization described by $\dot{K}^{xz} = -\sqrt{2}\alpha_\omega\mu_I^{xzxy}E(\omega)^2E(2\omega) \sin(2\phi_\omega - \phi_{2\omega})$, the spin-polarized electrical current in the y direction is described by $J^y = -2\alpha_\omega\text{Im}(\eta_I^{xyxy})E(\omega)^2E(2\omega) \cos(2\phi_\omega - \phi_{2\omega})$, and $\dot{K}^{yz} = -\{\mu_I^{xzxy} - \mu_I^{zyyy}\}E(\omega)^2E(2\omega) \cos(2\phi_\omega - \phi_{2\omega})$.

In the configuration where two colinearly polarized field $\mathbf{E}(\omega/2\omega) = E(\omega/2\omega)e^{i\phi_{\omega/2\omega}}\hat{\mathbf{x}}$ is incident on the quantum well, the electrical current due to interference of the ω and 2ω beams is in the x direction, $\mathbf{J} = -2\text{Im}[\eta_I^{xxxx}(\omega)]E(\omega)^2E(2\omega) \sin(2\phi_\omega - \phi_{2\omega})\hat{\mathbf{x}}$, while there is a pure spin current with average spin pointing along the growth axis and injected along y ; this pure spin current is represented by $\dot{K}^{yz} = 2\mu_I^{zyyy}E(\omega)^2E(2\omega) \cos(2\phi_\omega - \phi_{2\omega})$.

V. CONCLUSIONS

We have shown that quantum interference between one- and two-photon excitations in a quantum well semiconductor structure can be used to optically inject electrical and spin currents in the plane of an unbiased quantum well. The di-

rection of injection can be coherently controlled via the relative phase of the optical fields. The spin currents can be injected with or without an accompanying electrical current. Different polarization and direction of propagation of one or both optical fields allow many different possibilities of injection characteristics such as direction and spin properties.

The properties of the injected electrons in the plane of a GaAs quantum well were characterized. The average velocity with which electrons are injected can be a few hundreds of km/s, comparable to the swarm velocities with which electrons can be injected in bulk GaAs as well.²¹

The degree of spin polarization of the injected spin currents in a quantum well is significantly higher than in bulk GaAs and can be close to 100%. This is due to the splitting of the heavy- and light-hole subbands by dimensional confinement of the quantum well. This splitting can be maintained for energies well above the band gap in the presence of strain, which can result from lattice mismatch across the boundaries of the quantum well. The effects of a 2% biaxial compressive strain on the injected electrical and spin currents were detailed. The rearrangement of the quantum well subbands due to strain results in a high-spin polarization of the injected spin currents for photon energies well above the band gap. For an unstrained quantum well and photon energies close to the band gap, the velocity of the injected electrons is low, but the degree of spin polarization is highest; as the photon excitation energy increases, the velocity of the injected electrons increases, but the degree of spin polarization decreases. We found that in the case of a biaxially compressed quantum well one can have both high injection velocities, of the order of a few hundreds of km/s, and a high degree of spin polarization as well. This provides a unique opportunity for studying charge and spin transport in unbiased semiconductor nanostructures. The issues addressed here can be extended to other nanostructures, such as quantum wires.

ACKNOWLEDGMENTS

We thank Art Smirl, Henry van Driel, Oleg Prepelita, and Yaser Kearachian for useful discussions. This work was supported by DARPA, the Natural Sciences and Engineering Research Council of Canada, and Photonics Research Ontario. A.N. acknowledges support from an Ontario Graduate Scholarship and the Walter C. Sumner Foundation.

¹M. I. Dyakonov and V. I. Perel, in *Optical Orientation*, edited by F. Meier and B. P. Zakharchenya, *Modern Problems in Condensed Matter Sciences*, Vol. 8 (North-Holland, Amsterdam, 1984), Chap. 2.

²D. Hägele *et al.*, *Appl. Phys. Lett.* **73**, 1580 (1998).

³J. M. Kikkawa and D. D. Awschalom, *Nature (London)* **397**, 139 (1999).

⁴E. L. Ivchenko and G. E. Pikus, *Superlattices and Other Heterostructures* (Springer-Verlag, Berlin, 1997), Chap. 9.

⁵R. D. R. Bhat and J. E. Sipe, *Phys. Rev. Lett.* **85**, 5432 (2000).

⁶Martin J. Stevens, Arthur L. Smirl, R. D. R. Bhat, Ali Najmaie, J. E. Sipe, and H. M. van Driel, *Phys. Rev. Lett.* **90**, 136603 (2003).

⁷J. Hübner, W. W. Rühle, M. Klude, D. Hommel, R. D. R. Bhat, J. E. Sipe, and H. M. van Driel, *Phys. Rev. Lett.* **90**, 216601 (2003).

⁸J. M. Luttinger and W. Kohn, *Phys. Rev.* **97**, 869 (1955).

⁹J. P. Leohr, *Physics of Strained Quantum Well Lasers* (Kluwer Academic, Dordrecht, 1998), Chap. 3.

¹⁰For a cube of size a , the (001) biaxial strain corresponds to the

application of a stress across the xz and yz faces. The xy plane is a new square of length a' on each side. For an in-plane compression (stretch) of the cube, the cube expands (shrinks) vertically, thus producing a rectangular prism.

- ¹¹Lucio Claudio Andreani *et al.*, Phys. Rev. B **36**, 5887 (1987).
- ¹²The split-off subbands could nevertheless serve as intermediate states in multiphoton transitions. Using the 4×4 Luttinger-Kohn model for light and heavy holes and uncoupled sets of states for the conduction and split-off states, velocity matrix elements between heavy- or light-hole states and the split-off states strictly vanish. Therefore the contributions of split-off subbands as intermediate states to the quantities calculated in this paper vanish. Those elements do survive, however, in a more realistic model of the valence subbands. Using such a model for bulk GaAs, calculations show that contributions to injected electrical and spin currents from terms involving split-off bands as intermediate states only become important when, in the absence of their inclusion, a near-cancellation arises between terms involving heavy- and light-hole bands as initial states (Ref. 13). In the case of quantum wells subject to photons of the energies considered here electrons are optically injected into conduction subbands predominantly from heavy hole subbands. Hence, for the kind of initial study we present in this paper, we expect the neglect of split-off subbands as intermediate states should be a good approximation.
- ¹³R. D. R. Bhat and J. E. Sipe (unpublished).

- ¹⁴M. Lax, *Symmetry Principles in Solid State and Molecular Physics* (Wiley, New York, 1974), Chap. 10.
- ¹⁵Y.-C. Chang and R. B. James, Phys. Rev. B **39**, 12 672 (1989).
- ¹⁶F. Szmulowicz, Phys. Rev. B **51**, 1613 (1995); JETP Lett. **60**, 751 (1994).
- ¹⁷R. Atanasov *et al.*, Phys. Rev. Lett. **76**, 1703 (1996).
- ¹⁸A. Haché *et al.*, Phys. Rev. Lett. **78**, 306 (1997).
- ¹⁹N. Laman *et al.*, Appl. Phys. Lett. **75**, 2581 (1999).
- ²⁰M. SheikBahae, Phys. Rev. B **60**, R11 257 (1999).
- ²¹*Ultrafast Phenomena in Semiconductors*, edited by Kong-Thon Tsen (Springer, Berlin, 2001), Chap. 5.
- ²²M. J. Stevens *et al.*, J. Appl. Phys. **91**, 4382 (2002).
- ²³24 E. Dupont *et al.*, Phys. Rev. Lett. **74**, 3596 (1995).
- ²⁴25 P. Král and J. E. Sipe, Phys. Rev. B **61**, 5381 (2000).
- ²⁵Y. Ohno, R. Terauchi, T. Adachi, F. Matsukura, and H. Ohno, Phys. Rev. Lett. **83**, 4196 (1999).
- ²⁶J. M. Fraser *et al.*, Phys. Rev. Lett. **83**, 4192 (1999).
- ²⁷J. E. Sipe and A. I. Shkrebtii, Phys. Rev. B **61**, 5337 (2000).
- ²⁸S. D. Ganichev, E. L. Ivchenko, S. N. Danilov, J. Erms, W. Wegscheider, D. Weiss, and W. Prettl, Phys. Rev. Lett. **86**, 4358 (2001).
- ²⁹G. L. Bir and G. E. Pikus, *Symmetry and Strained-Induced Effects in Semiconductors* (Wiley, New York, 1974).
- ³⁰For a given photon energy and angle ϕ , the total spin injection $|\bar{S}^z(\phi)|$ (17) must be less than $\hbar/2$.
- ³¹This argument holds for all the experimental configurations considered in this paper (Figs. 5, 8 and 11).